Geochemical Perspectives Letters

In situ determination of sulfur speciation and partitioning in aqueous fluid-silicate melt systems

A. Colin[1], C. Schmidt[2], G.S. Pokrovski[1*], M. Wilke[3], A.Y. Borisova[1,4], M.J. Toplis[5]

doi: 10.7185/geochemlet.2020

Abstract

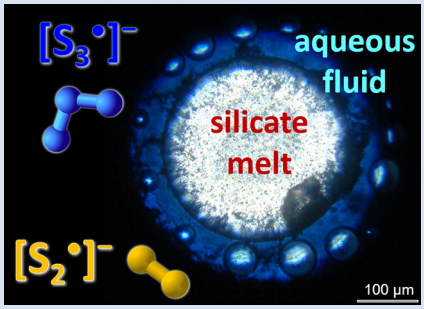

Current knowledge of sulfur behaviour in magmas is based exclusively on *ex situ* analyses. Here we report the first *in situ* measurement of sulfur speciation and partitioning between coexisting aqueous fluids and silicate melts. These data were acquired using Raman spectroscopy in a diamond anvil cell at 700 °C, 0.3–1.5 GPa, and oxygen fugacity in the vicinity of the sulfide-sulfate transition, conditions relevant to subduction zone magmatism. Results show that sulfate and sulfide are dominant in the studied systems, together with the $S_3^{\bullet-}$ and $S_2^{\bullet-}$ radical ions that are absent in quenched fluid and silicate glass products. The derived fluid/melt partition coefficients for sulfide and sulfate are consistent with those from available *ex situ* data for shallow crust conditions (<10 km), but indicate stronger partitioning of these sulfur species into the silicate melt phase with increasing depth. In contrast, both radical ions partition at least 10 times more than sulfate and sulfide into the fluid phase. Thus, by enhancing the transfer of sulfur and associated chalcophile metals from melt into fluid upon magma degassing, $S_3^{\bullet-}$ and $S_2^{\bullet-}$ may be important players in the formation of economic metal resources within the redox window of the sulfate-sulfide transition in subduction zone settings.

Received 11 September 2019 | Accepted 23 May 2020 | Published 10 July 2020

Introduction

The solubility, partitioning, and chemical speciation of sulfur in aqueous fluid-silicate melt systems are controlling factors in the processes of volatile and metal transfer and ore deposit formation in geodynamic settings associated with subduction zones. Our knowledge of these factors is currently based on *ex situ* analyses of fluids and melts brought to the Earth's surface or recovered in laboratory experiments upon cooling, such as volcanic sublimates and gases, fluid inclusions or silicate glasses. Yet, the complex and highly variable chemical and redox states of sulfur, spanning from S^{2-} (sulfide) to S^{6+} (sulfate), raise questions of how stable the different sulfur species are at temperatures (T) and pressures (P) relevant to magma generation and evolution, and how representative quenched natural and experimental samples are with regard to sulfur speciation and partitioning across the lithosphere. Indeed, along with coexisting sulfate and sulfide commonly observed in quenched samples, other previously disregarded species such as the tri- and disulfur radical ions, $S_3^{\bullet-}$ and $S_2^{\bullet-}$, become increasingly abundant in aqueous fluids above 200 °C but cannot be preserved upon cooling being unstable at ambient conditions (Pokrovski and Dubrovinsky, 2011; Schmidt and Seward, 2017). On the other hand, these radicals can bind to gold in hydrothermal fluids thereby enhancing the efficiency of gold supply to ore deposits (Pokrovski *et al.*, 2015; 2019). At shallow crust conditions (<0.3 GPa, <10 km depth), porphyry Cu-Mo-Re-Au and associated epithermal and skarn deposits, which are among the most significant resources of those metals on Earth, form in the vicinity of degassing magma bodies emplaced in the upper continental crust of arcs and back arc settings (Hedenquist and Lowenstern, 1994; Fontboté *et al.*, 2017). Although available natural silicate glass analyses, experimental data, and resulting models for sulfur in hydrous silicate melts provide a robust understanding of sulfur redox and partitioning at such conditions (*e.g.*, Moretti and Baker, 2008; Klimm and Botcharnikov, 2010; Wallace and Edmonds, 2011; Zajacz *et al.*, 2012; Zajacz, 2015; Binder *et al.*, 2018), much less is known about S redox and distribution in fluid-melt systems from lower crustal and upper mantle settings relevant to magma generation in subduction zones from which water, sulfur and metals for these deposits are sourced. At such depths (30–100 km, ~1–3 GPa), dehydration of the subducting slab generates aqueous fluids that can cause partial melting of the overlying mantle wedge (Hedenquist and Lowenstern, 1994; Richards, 2003). Such melts that become fluid saturated at some depth may carry and release significant amounts of

1. Group Fluids at Extreme Conditions (FLEX), Géosciences Environnement Toulouse (GET), Observatoire Midi-Pyrénées, Centre National de la Recherche Scientifique (CNRS), UMR 5563, Université de Toulouse, Institut de Recherche pour le Développement (IRD), 14 avenue Edouard Belin, 31400 Toulouse, France
2. Deutsches GeoForschungsZentrum (GFZ), Telegrafenberg, 14473 Potsdam, Germany
3. Universität Potsdam, Institut für Geowissenschaften, 14476 Potsdam, Germany
4. Geological Department, Lomonosov Moscow State University, Vorobievy Gory, 119899, Moscow, Russia
5. Institut de Recherche en Astrophysique et Planétologie (IRAP), Observatoire Midi-Pyrénées, Centre National de la Recherche Scientifique (CNRS), Université de Toulouse, 9 Avenue du Colonel Roche, 31400 Toulouse, France

* Corresponding author (email: gleb.pokrovski@get.omp.eu; glebounet@gmail.com)

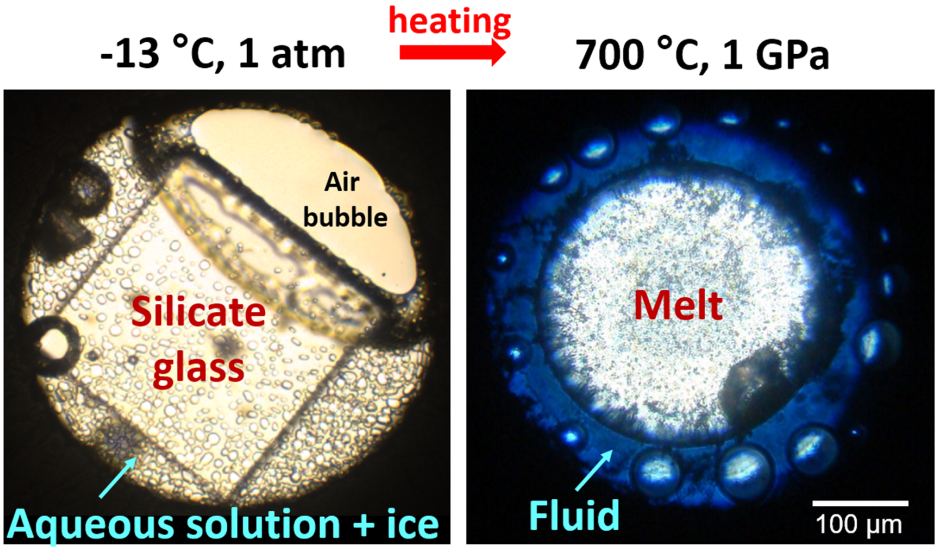

Figure 1 *In situ* approach applied in this study to determine sulfur speciation and partitioning in fluid-magma systems. A chip of silicate glass and aqueous thiosulfate solution are loaded in a diamond anvil cell (left), which is then heated to 700 °C and 0.3–1.5 GPa yielding a silicate melt and a blue aqueous fluid containing significant amounts of trisulfur radical ion (right). The coexisting phases are directly probed by micro-Raman spectroscopy and quantification based on Raman band intensities was performed using a method developed in this study (Supplementary Information).

sulfur-bound metals such as Au, Cu and Mo, whose fate strongly depends on the redox state and partitioning of sulfur itself between fluid and melt, during magma storage, evolution and transport across the subduction zone (*e.g.*, Richards, 2003; Audétat and Simon, 2012; Chelle-Michou *et al.*, 2017).

In an attempt to probe directly the sulfur chemical speciation and partitioning at the magmatic-hydrothermal transition, and to assess the impact of non-quenchable sulfur species such as $S_3^{\bullet-}$ and $S_2^{\bullet-}$ that cannot be studied using *ex situ* methods, we applied an *in situ* approach. Our method is based on Raman spectroscopy in a diamond anvil cell (DAC) and provides an unprecedented direct "window" into the identity, amount, and distribution of S species in fluid-magma systems (Supplementary Information). Here, we examined a set of four natural and synthetic silicate glasses, with SiO_2 contents from 50 to 75 mass % and alkalinity (Na + K)/Al (mol) from 0.6 to 3.0 (Tables S-1, S-2). Their composition has been chosen in this exploratory study to respond to three principal criteria: i) experimental feasibility, ii) relevance to the conditions of magma generation in subduction zones, and iii) possibility to cover a large range of silica content and alkalinity that are the major parameters controlling sulfur partitioning as seen by *ex situ* studies. The melts generated upon heating were equilibrated with sulfide/sulfate-bearing aqueous solutions at 700 °C and 0.3–1.5 GPa (Fig. 1).

Sulfur Speciation in the Coexisting Fluid and Melt Phases

Raman spectroscopy is the method of choice to study different sulfur species in fluids and melts owing to their characteristic and intense Raman scattering bands (Schmidt and Seward, 2017). The fluid phase at high *T-P* in all DAC experiments (Table S-2) shows Raman bands of water, dissolved silica species, and sulfate and sulfide (Fig. 2). In experiments with both sulfate and sulfide, the fluid displays a blue colour under white light illumination (Fig. 1), demonstrating the presence of the blue chromophore $S_3^{\bullet-}$ ion (Chivers and Elders, 2013). The Raman spectrum of the fluid phase indeed shows the characteristic

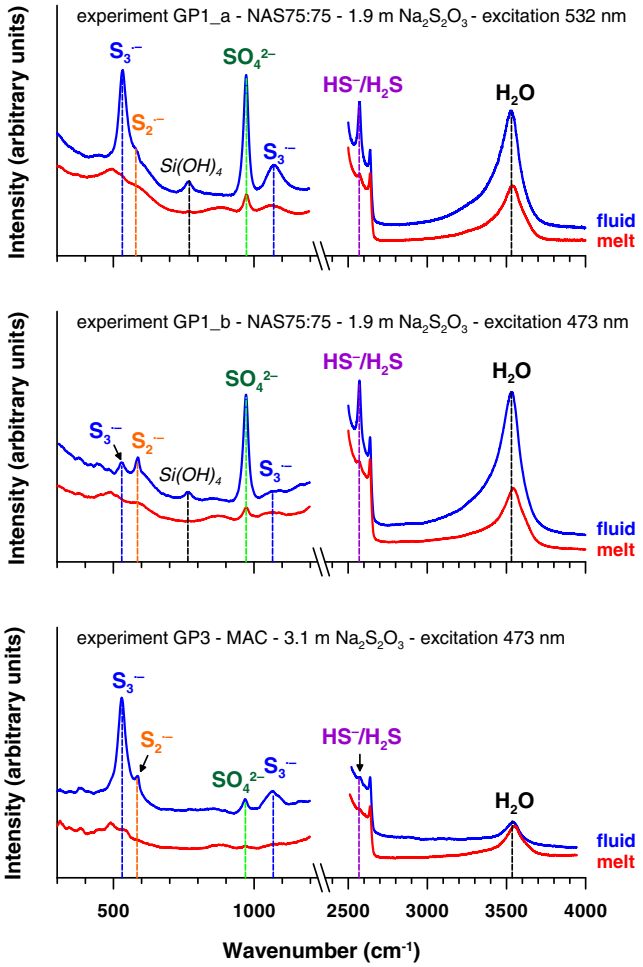

Figure 2 Raman spectra from representative experiments with indicated fluid and melt compositions, acquired at 700 °C and ~1 GPa with 473 and 532 nm excitation, and the major identified species.

vibrations of $S_3^{\bullet-}$ and $S_2^{\bullet-}$ ions, with signal intensity from $S_2^{\bullet-}$ increasing relative to that from $S_3^{\bullet-}$ in fluids in equilibrium with more alkaline melts (Fig. 2), in agreement with the reactions of $S_2^{\bullet-}$ and $S_3^{\bullet-}$ formation that are favoured at low and high proton activity, respectively:

$$13H_2S_{(aq)} + 3SO_4^{2-} = 8S_2^{\bullet-} + 2H^+ + 12H_2O_{(liq)} \quad \text{Eq. 1}$$

$$19H_2S_{(aq)} + 5SO_4^{2-} + 2H^+ = 8S_3^{\bullet-} + 20H_2O_{(liq)} \quad \text{Eq. 2}$$

The O–H stretching band of water in the spectra of silicate melts differs both in shape and position from that in spectra of the coexisting aqueous fluid. The melt spectra also show low intensity Si–O and Si–O–Si bands, similar to those in quenched glasses but distinct from those in the aqueous fluid (Figs. 2, S-3), thus supporting a negligible contribution of the fluid to the melt spectra. The species H_2S (and HS^-) and SO_4^{2-} are systematically detected in the silicate melt. The Raman signal from $S_3^{\bullet-}$ in the melt was quantified in two experiments (those with the highest S concentrations of >10 mass % S), whereas $S_3^{\bullet-}$ from S-poor experiments and $S_2^{\bullet-}$ in melts from all experiments were below detection (Figs. S-2, S-3, Table S-2).

In Situ Fluid/Melt Partition Coefficients of Sulfur Species

Our *in situ* data allow generation of the first direct set of fluid/melt partition coefficients, $D^{fl/mt}$(i), of each individual S species (where i = sulfate, sulfide, $S_3^{\bullet-}$, or $S_2^{\bullet-}$; Fig. 3, Table S-5). The $D^{fl/mt}$(sulfate) values are constant within measurement analytical uncertainties (1 standard deviation, s.d.) among the four studied melts, with an average of 17 ± 8 (1 s.d. of the mean) at 700 °C and 0.3–1.5 GPa, whereas the $D^{fl/mt}$(sulfide) values range from 6 ± 2 to 28 ± 8 (1 s.d.) from peraluminous to peralkaline melts, respectively (Fig. 3). Remarkably, the minimum $D^{fl/mt}$ values of both radical ions (50–450; Fig. 3) are at least a factor of 10 higher in favour of the fluid phase than those of sulfate and sulfide (see Supplementary Information for details of quantification). Thus, our *in situ* data reveal a much higher affinity of both radicals for the fluid phase compared to sulfate and sulfide, an important new finding that cannot be obtained using *ex situ* methods (see Supplementary Information for comparison with *ex situ* data).

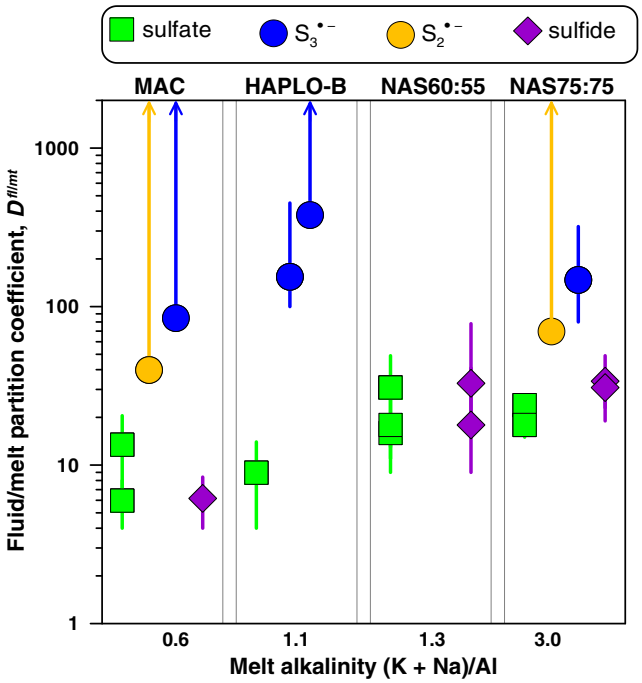

Figure 3 Partition coefficients (defined as the ratio of the species concentration in the fluid over its concentration in the silicate melt) at 700 °C and 0.3–1.5 GPa between fluid and melt for each sulfur species ($S_2^{\bullet-}$, $S_3^{\bullet-}$, sulfate and sulfide) for the indicated silicate melt compositions as a function of the initial alkalinity (Tables S-1, S-5; error bars 1 s.d.). Data points for the radical ions accompanied by arrowed vertical bars are minimal estimates corresponding to their detection limit in the melt.

Sulfur and Metal Transfer from Magmas to Ore Deposits in Subduction Zones

Our new findings provide insight into sulfur behaviour in subduction zone settings where fluid saturated melt generation, transfer and degassing can occur across a wide range of *T-P* and depth.

Firstly, our novel *in situ* data offer the advantage of direct estimation of sulfide and sulfate $D^{fl/mt}$ values for a given melt composition across a large f_{O2} range, because fluid/melt partitioning of an individual sulfur species is independent of f_{O2}. Our extrapolated values for melts of rhyolitic composition equilibrated with aqueous fluids at 0.3–1.5 GPa ($D^{fl/mt}$(sulfate) ~10 and $D^{fl/mt}$(sulfide) <10; Figs. 4, S-5) are a factor of 10 lower than those inferred from *ex situ* experiments performed at pressures of <0.5 GPa (see Supplementary Information) and analyses of natural glass inclusions trapped in volcanic rocks (*e.g.*, Wallace and Edmonds, 2011). Our results imply that felsic magmas, generated at depth and degassing through the lithosphere (10–45 km) both at highly reducing and highly oxidising conditions (*i.e.* outside the f_{O2} range within which the radical ions may be abundant), may retain more sulfur than was expected from *ex situ* analyses.

Secondly, our results demonstrate that both $S_2^{\bullet-}$ and $S_3^{\bullet-}$ ions are abundant in the S-rich fluid phase at the f_{O2} range of the sulfide-sulfate transition at temperatures of magma generation. First order estimates of the $S_3^{\bullet-}$ fraction in the experimental fluids of this study (700 °C, 1 GPa, 1–4 molal $Na_2S_2O_3$), amounting from 5 to 50 % of S_{tot}, are in good agreement with that predicted (Fig. S-8) using recent thermodynamic models based on *in situ* data at ≲500 °C (Pokrovski and Dubessy, 2015). The f_{O2} range favourable for both radicals matches that of the mantle wedge above the subducting slab where partial melting occurs. At these depths, back and forth changes in f_{O2} across the sulfate-sulfide transition window are common (Fig. 4). For instance, sulfate-dominated fluids, derived from subducted oceanic crust at >100 km depth, have the ability to oxidise the sulfide-bearing mantle wedge (*e.g.*, Evans, 2012; Walters *et al.*, 2020), by producing partial melts that rise up further to the mantle-crust boundary (70–40 km depth) and experience multiple phenomena (*e.g.*, Richards, 2003; Evans, 2012) as outlined in Figure 4. At higher crustal levels (5–15 km depth), mixing between sulfate-bearing felsic and FeS-bearing mafic melts may lead to S-rich magmas and fluids that are the major source of Au, Cu and Mo in porphyry deposits (Audétat and Simon, 2012). At shallower depths (<5 km), conduit flow modelling shows that degassing magmas rising to the surface in arc settings may evolve from reduced to oxidised, or oxidised to reduced, depending on their S content and initial f_{O2} (Burgisser and Scaillet, 2007). In summary, at different stages of their evolution, arc magmas are likely to cross the sulfide-sulfate transition

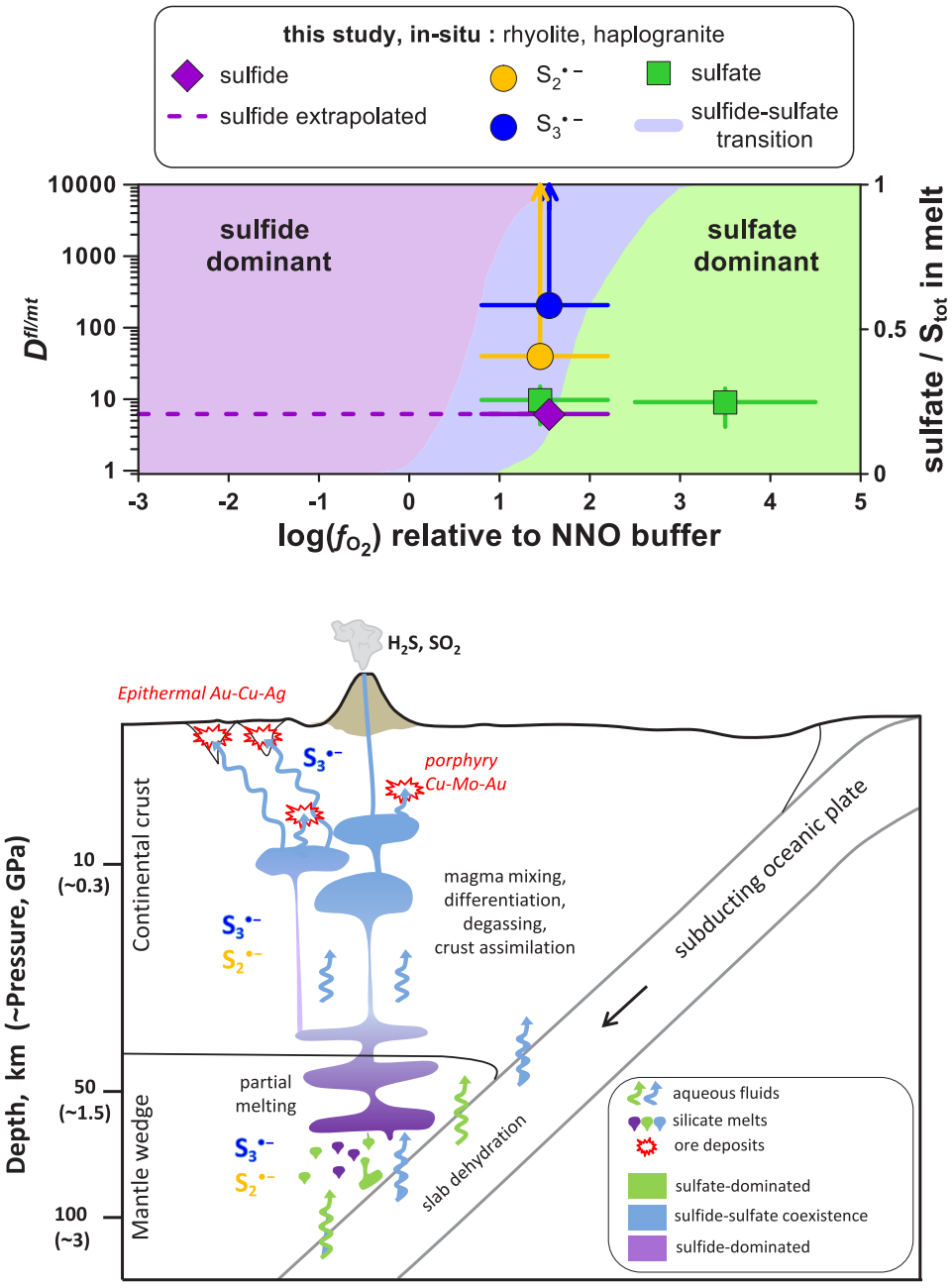

Figure 4 (Upper panel) *In situ* fluid/melt partition coefficients of sulfate, sulfide, $S_3^{\bullet-}$ and $S_2^{\bullet-}$, derived in this study for felsic melts (MAC, HAPLO-B) at 700 °C and 0.3–1.5 GPa as a function of f_{O2} (error bars 1 s.d.). Blue area outlines the sulfate-sulfide boundary in water saturated melt (Moretti and Baker, 2008); horizontal dashed line shows partition coefficients of sulfide extrapolated to the more reduced conditions of our *in situ* measurements. (Lower panel) Cartoon of a subduction zone setting (not to scale) schematically illustrating silicate melt and aqueous fluid generation and evolution, and the associated sulfur redox changes.

favouring formation of $S_2^{\bullet-}$ and $S_3^{\bullet-}$ (Fig. 4). Both radical ions partition at least 10 times more than sulfide and sulfate from felsic magmas into the volatile aqueous phase, thereby potentially enhancing sulfur degassing, depending on the initial fraction of sulfur in the form of radical ions in the melt (Fig. S-7) and total S content (S_{tot}) in the system (Fig. S-8), because $S_2^{\bullet-}$ and $S_3^{\bullet-}$ respective abundances are roughly a square and a cubic function of S_{tot}.

Thirdly, the strong enrichment of the fluid in radical ions compared to melt, coupled with the high affinity of $S_3^{\bullet-}$ and $S_2^{\bullet-}$ for gold (*e.g.*, Pokrovski *et al.*, 2019), and potentially for critical metals that have strong chemical bonds with sulfur (Pt, Pd, Mo, Re; *e.g.*, Laskar *et al.*, 2019), may be a key factor controlling trace metal transfer from the melt to the S-bearing fluid. Gold solubility in silicate melts displays a maximum at S^{6+}/S^{2-} ratios between 0.1 and 0.9 (Botcharnikov *et al.*, 2011; Zajacz *et al.*, 2012), implying enhanced gold extraction from the mantle by magmas generated by partial melting of the mantle wedge at such redox conditions. Upon ascent and degassing of such Au pre-enriched magma, this gold is remobilised and concentrated by the released $S_3^{\bullet-}$-bearing fluids. According to Eqs. 1 and 2, the concentrations of the di- and trisulfur ions are maximised both in melt and fluid at sulfide:sulfate ratios of 13:3 and 19:5, respectively (corresponding to ~80 % of S_{tot} as sulfide). Such sulfide-dominated, yet moderately oxidised, systems are common in arc magma settings that host major porphyry-epithermal

Cu-Mo-Au deposits (Fontboté *et al.*, 2017). According to the most conservative estimates of the $D^{fl/mt}(S_3^{\bullet-})$ values in this study (~100), a melt containing only 10 µg/g S in the form of $S_3^{\bullet-}$ would produce 1000 µg/g S as $S_3^{\bullet-}$ in the fluid at equilibrium. Such concentrations of trisulfur ion are largely sufficient to bind to trace metals, extract them from the magma, transport them in the fluid phase to ore deposition sites, and control the deposition due to $S_3^{\bullet-}$ destabilisation upon fluid cooling, boiling or interaction with rocks. Our study thus reveals that sulfur radical ions may be key players in the formation of economic metal resources within the redox window of the sulfate-sulfide transition across subduction zone settings.

Acknowledgements

This work was funded by the French National Research Agency (grants RadicalS, ANR-16-CE31-0017), the Institut Carnot ISIFoR (grant OrPet), and the French and German embassies (grant PHC Procope SulFluMag). We thank T. Aigouy, P. Besson, J. Buhk, A. Castillo, P. Gisquet, S. Gouy, M. Kokh, J.-F. Ména, F. de Parseval, P. de Parseval, and S. Moyano for their help with sample preparation and analyses, A.-M. Cousin for her help with figure layout, W.A. Bassett for advice on DAC techniques, G. Harlow, J. Newman and B. Ledé for providing lazurite samples, and K. Kiseeva for discussions. Constructive comments of Editor H. Marschall and reviewers Z. Zajacz and C. LaFlamme greatly improved this article. We are grateful to A. Williams and M.-A. Hulshoff for editorial management.

Editor: Horst R. Marschall

Additional Information

Supplementary Information accompanies this letter at http://www.geochemicalperspectivesletters.org/article2020.

Cite this letter as: Colin, A., Schmidt, C., Pokrovski, G.S., Wilke, M., Borisova, A.Y., Toplis, M.J. (2020) *In situ* determination of sulfur speciation and partitioning in aqueous fluid-silicate melt systems. *Geochem. Persp. Let.* 14, 31–35.

References

Audétat, A., Simon, A.C. (2012) Magmatic controls on porphyry copper genesis. *Society of Economic Geologists Special Publication* 16, 553–572.

Binder, B., Wenzel, T., Keppler, H. (2018) The partitioning of sulfur between multicomponent aqueous fluids and felsic melts. *Contribution to Mineralogy and Petrology* 173, 18.

Botcharnikov, R., Linnen, R.L., Wilke, M., Holtz, F., Jugo, P.J., Berndt, J. (2011) High gold concentrations in sulphide-bearing magma under oxidizing conditions. *Nature Geoscience* 4, 112–115.

Burgisser, A., Scaillet, B. (2007) Redox evolution of a degassing magma rising to the surface. *Nature* 445, 194–197.

Chelle-Michou, C., Rottier, B., Caricchi, L., Simpson, G. (2017) Tempo of magma degassing and the genesis of porphyry copper deposits. *Scientific Reports* 7, 40566.

Chivers, T., Elder, P.J.W. (2013) Ubiquitous trisulfur radical ion: fundamentals and applications in materials science, electrochemistry, analytical chemistry and geochemistry. *Chemical Society Reviews* 42, 5996–6005.

Evans, K.A. (2012) The redox budget of subduction zones. *Earth Science Reviews* 113, 11–32.

Fontboté, L., Kouzmanov, K., Chiaradia, M., Pokrovski, G.S. (2017) Sulfide minerals in hydrothermal deposits. *Elements* 13, 97–103.

Hedenquist, J.W., Lowenstern, J.B. (1994) The role of magmas in the formation of hydrothermal ore deposits. *Nature* 370, 519–527.

Klimm, K., Botcharnikov, R.E. (2010) The determination of sulfate and sulfide species in hydrous silicate glasses using Raman spectroscopy. *American Mineralogist* 95, 1574–1579.

Laskar, C., Pokrovski, G.S., Kokh, M.A., Hazemann, J.-L., Bazarkina, E.F., Desmaele, E. (2019) The impact of sulfur on the transfer of platinoids by geological fluids. *Abstracts of the Goldschmidt 2019 Conference, Barcelona, Spain*, 1831 (hal-02343794).

Moretti, R., Baker, D.R. (2008) Modeling the interplay of fO_2 and fS_2 along the FeS-silicate melt equilibrium. *Chemical Geology* 256, 286–298.

Pokrovski, G.S., Dubrovinsky, L.S. (2011) The S_3^- ion is stable in geological fluids at elevated temperatures and pressures. *Science* 331, 1052–1054.

Pokrovski, G.S., Dubessy, J. (2015) Stability and abundance of the trisulfur radical ion in hydrothermal fluids. *Earth and Planetary Science Letters* 411, 298–309.

Pokrovski, G.S., Kokh, M.A., Guillaume, D., Borisova, A.Y., Gisquet, P., Hazemann, J.-L., Lahera, E., Del Net, W., Proux, O., Testemale, D., Haigis, V., Jonchière, R., Seitsonen, A.P., Ferlat, G., Vuilleumier, R., Saitta, A.M., Boiron, M.-C., Dubessy, J. (2015) Sulfur radical species form gold deposits on Earth. *Proceeding of the National Academy of Sciences of the U.S.A.* 112, 13484–13489.

Pokrovski, G.S., Kokh, M.A., Proux, O., Hazemann, J.-L., Bazarkina, E.F., Testemale, D., Escoda, C., Boiron, M.-C., Blanchard, M., Ajgouy, T., Gouy, S., de Parseval, P., Thibaut, M. (2019) The nature and partitioning of invisible gold in the pyrite-fluid system. *Ore Geology Reviews* 109, 545–563.

Richards, J.P. (2003) Tectono-magmatic precursors for porphyry Cu-(Mo-Au) deposit formation. *Economic Geology* 98, 1515–1533.

Schmidt, C., Seward, T.M. (2017) Raman spectroscopic quantification of sulfur species in aqueous fluids: Ratios of relative molar scattering factors of Raman bands of H_2S, HS^-, SO_2, HSO_4^-, SO_4^{2-}, $S_2O_3^{2-}$, S_3^- and H_2O at ambient conditions and information on changes with pressure and temperature. *Chemical Geology* 467, 64–75.

Wallace, P.J., Edmonds, M. (2011) The sulfur budget in magmas: evidence from melt inclusions, submarine glasses and volcanic emissions. *Reviews in Mineralogy and Geochemistry* 73, 215–246.

Walters, J.B., Cruz-Uribe, A.M., Marschall, H.R. (2020) Sulfur loss from subducted altered crust and implications for mantle oxidation. *Geochemical Perspectives Letters* 13, 36–41.

Zajacz, Z. (2015) The effect of melt composition on the partitioning of oxidized sulfur between silicate melts and magmatic volatiles. *Geochimica et Cosmochimica Acta* 158, 223–244.

Zajacz, Z., Candela, P.A., Piccoli, P.M., Wälle, M., Sanchez-Valle, C. (2012) Gold and copper in volatile saturated mafic to intermediate magmas: Solubilities, partitioning, and implications for ore deposit formation. *Geochimica et Cosmochimica Acta* 91, 140–159.